Establishing a tracer-based sediment budget to preserve wetlands in Mediterranean mountain agroecosystems (NE Spain)

Ana Navas[a*], Manuel López-Vicente[a], Leticia Gaspar[b], Leticia Palazón[a], Laura Quijano[a]

[a]*Department of Soil and Water, Estación Experimental de Aula Dei, EEAD-CSIC, Avda. Montañana 1005, 50059 Zaragoza, Spain.*

[b] *School of Geography, Earth and Environmental Science, Plymouth University, Plymouth, Devon PL4 8AA, UK*

[*]anavas@eead.csic.es, mvicente@eead.csic.es, leticia.gaspar@plymouth.ac.uk, lpalazon@eead.csic.es, lquijano@eead.cisc.es

[*] Corresponding author. E-mail address: anavas@eead.csic.es Postal address: Avda. Montañana 1005 – 50059 Zaragoza, Spain. Telephone number: (34) 976 716 094. Fax number: (34) 976 716 145

Abstract

Mountain wetlands in Mediterranean regions are particularly threatened in agricultural environments due to anthropogenic activity. An integrated study of source-to-sink sediment fluxes was carried out in an agricultural catchment that holds a small permanent lake included in the European NATURA 2000 Network. More than 1,000 years of human intervention and the variety of land uses pose a substantial challenge when attempting to estimate sediment fluxes which is the first requirement to protect

fragile wetlands. To date, there have been few similar studies and those that have been carried out have not addressed such complex terrain. Geostatistical interpolation and GIS tools were used to derive the soil spatial redistribution from point ^{137}Cs inventories, and to establish the sediment budget in the catchment located in the Southern Pyrenees. The soil redistribution was intense and soil erosion predominated over soil deposition. On the areas that maintained natural vegetation the median soil erosion and deposition rates were moderate, ranging from 2.6 to 6 Mg ha yr^{-1} and 1.5 to 2.1 Mg ha yr^{-1}, respectively. However, in cultivated fields both erosion and deposition were significantly higher (ca. 20 Mg ha yr^{-1}), and the maximum rates were always associated with tillage practices. Farming activities in the last part of the 20th century intensified soil erosion, as evidenced by the 1963 ^{137}Cs peaks in the lake cores and estimates from the sediment budget indicated a net deposition of 671 Mg yr^{-1}. Results confirm a siltation risk for the lake and provide a foundation for designing management plans to preserve this threatened wetland. This comprehensive approach provides information useful for understanding processes that influence the patterns and rates of soil transfer and deposition within fragile Mediterranean mountain wetlands subjected to climate and anthropogenic stresses.

Key words: Soil redistribution; ^{137}Cs; GIS; lake siltation; sediment dating; endorheic agroforestry catchment; karstic.

1. Introduction

Human activities over past centuries have been the main drivers of transformations in ecosystems by converting natural landscapes into agricultural land. Since the first

agricultural settlements in the Western Mediterranean around 6000-7000 BP (Manen and Sabatier, 2003), the creation of agricultural lands and the overexploitation of forests have accelerated in some places the processes of soil loss and degradation (García-Ruiz, 2010). In the past decades, the anthropogenic impact has triggered important changes in land uses, and the associated risk of cycles of land abandonment and return to cultivation has posed threats to soil and water sustainability in fragile Mediterranean sub-humid areas.

Wetlands in Mediterranean regions are especially fragile and there has been a gradual increase in the drastic retreat of such natural systems over the past century (Valero-Garcés et al., 2006). It is widely acknowledged that wetlands are important for water storage and purification, for carbon sequestration, and for the maintenance of biodiversity and wildlife habitats. Furthermore, wetlands provide ecosystem services, which are important to the welfare of society (Everard, 2004). Under conditions of climate change and because of its influence on earth surface processes it is necessary to investigate the relationships between driven controls such as climate, physiographic factors, land use and vegetation cover and erosion-deposition processes because the underlying processes are still poorly understood (Ruiz-Navarro et al., 2012).

One of the main environmental concerns worldwide is water pollution and further pressure on water resources is expected in the 21st century, which will exacerbate the threat to fragile wetland systems in the Mediterranean region. While cultivation is considered a key factor in promoting soil mobilization, related indirect effects of soil loss and transport of associated pesticides and fertilizers might contribute to contamination and siltation of wetland areas, thus damaging aquatic habitats. Undertaking conservation and restoration of wetlands is a major issue for environmental management in the context of Payment for Ecosystem Services policies (Everard,

2004), but to this end it is necessary to generate sound datasets.

Catchments constitute logical units for management of the water cycle (Everard, 2004), which is especially important for wetlands that are vital to ensure ecosystem functions. In recent years, the need for research into sediment dynamics in catchments has arisen due to a growing awareness of the environmental impact of the sediment loads on water resources (Porto et al., 2011).

Soil particle cycling involves soil particle generation, mobilization, intra-storage within catchments, and external transfer. Human activities have created numerous linear landscape elements (unpaved and paved trails, roads, land levelling, irrigation ditches, stone walls, dams, etc.) thus modifying the patterns of the overland flow and sediment connectivity (Borselli et al., 2008). Moreover, vegetation development and vegetation structure also affect the connectivity of runoff and soil redistribution processes on slopes (Cerdá, 1997). Thus, the interfacing of patches of different land uses and linear landscape elements modify soil redistribution processes and the sediment connectivity along the slopes affecting the final export of sediment (Gaspar et al., 2013, López-Vicente et al., 2013).

Spatially distributed estimates of soil redistribution rates within a catchment will lead to a better comprehension of the links between sediment mobilization, intrastorage and output (Porto et al. 2011). In this context the use of tracing techniques to provide spatially distributed information on the mobilization and transfer of sediments (Walling et al., 2006) is necessary for accurate assessment of siltation risks in water bodies.

Fallout ^{137}Cs has been effectively used to trace soil redistribution in diverse environments (Walling et al., 2006; Ritchie and McCarty, 2008; Mabit et al., 2008; Kato et al., 2010). The artificial radionuclide (half-life 30.2 year) was introduced in the stratosphere as a result of thermonuclear weapons test and its fallout started in 1954

with a peak in 1963, the year of the Nuclear Test Ban Treaty (IAEA, 1990). After rapid adsorption by clay minerals and organic matter (Tamura, 1964; Staunton et al., 2002) the redistribution of ^{137}Cs occurs in association with soil and sediment particles and is primarily controlled by its interaction with land use practices, erosion and sediment transport processes (Walling and He, 1999), although some ^{137}Cs can be mobilized by chemical and biological processes.

To identify the main factors triggering erosion, the sources of sediments and to quantify the risk of wetland siltation, analyses at the catchment scale provide a more comprehensive approach to the main control factors involved and facilitate an understanding of ecosystem functioning. However, despite their relevance for water storage, biodiversity conservation and ecosystem functioning, studies on mountain wetlands are scarce, particularly with regard to the Mediterranean region.

The Estanque Grande Catchment is an endorheic area that offers an exceptional opportunity to investigate soil redistribution patterns and to establish a sediment budget. To date, few attempts have been made to upscale data to catchment scale (Mabit et al., 2002; Porto et al., 2003; Mabit and Bernard, 2007; Navas et al., 2013), in spite of this being a key issue to understanding mobilization of sediments and their final export to water bodies (Porto et al., 2009). Evaluation of soil redistribution within the contributing catchment as the source and the sedimentation rate in the lake as the sink, using ^{137}Cs and GIS techniques, would allow a sediment budget to be established in a mountain wetland system. With this aim in mind, a combination of a radiotracer technique with a detailed physiographic database and high spatial resolution DEM within a GIS framework was used to map the medium-term soil erosion and deposition rates provided by fallout ^{137}Cs across the endorheic catchment and that of sediments finally reaching the lake. The overarching objectives of this study were to: i) examine

the patterns of soil redistribution, ii) establish the sediment budget, and iii) identify the main factors controlling sediment export to the lake under the current land use and climate scenario. The identification of source areas and sinks of sediments is of value to determine the risk of siltation of the central lake in the Estaña wetlands. Identifying patterns in the erosive process within this endangered wetland will develop information that will promote Estaña wetland conservation and that of other similar mountain wetlands located in agricultural areas.

2. Material and methods

2.1. *Study area: physiography, land uses and land cover*

The Estanque Grande Catchment is representative of mountain agroecosystems developed after centuries of human activity. This catchment containing a karstic lake in the southern part of the pre-Pyrenees, exemplifies the main features of Mediterranean wetlands. In the catchment changes in land uses have strongly modified landscapes by creating numerous linear landscape elements aimed at protecting the soil from erosion in an area of high rainfall intensity and steep slopes (López-Vicente et al., 2008b). The catchment (1.66 km^2) is characterized by abrupt topography with altitude ranging between 676 and 894 m above sea level (a.s.l). The endorheic catchment is included in a paleopolje, an extensive depression with no outflowing surface stream, which is located in the karstic region of the Pyrenean External Ranges close to the northern boundary of the Ebro Basin. It holds a permanent lake of 0.15 km^2 and a small pond, which at present is almost silt filled as well as several dolines or solution sinkholes (Fig.1 a). Since 1997 the wetland area has been under protection by the regional government and is included in the European NATURA 2000 Network as a Site of Community Importance (SCI). The lakes are fed by ground waters (IGME, 1982). The underlying

materials consist of gypsiferous marls, dolomites, limestones, ophites, and sparse saline deposits of Mesozoic and Neogene ages. Gypsiferous marls occupy mainly flat areas surrounding the lakes, which are under cultivation. Tillage practices in the vicinity of the lakes increases the risk of supplying sediment to the lakes as gypsiferous materials are highly erodible (Machín and Navas, 1998). There are no permanent rivers in the catchment and the hydrological network consists of 10 systems of gullies and 1 ephemeral gully system that in total occupy 17300 m^2 (Fig 1b). A characteristic feature of these systems is that none of the gullies inflows into the lake because they have been blocked and diverted at the entry to the agricultural areas surrounding the lake. The mean length of the gullies is 210 m with minimum and maximum lengths of 86 and 313 m, respectively. There is a strong topographic contrast between the slopes and the flat area surrounding the lakes. The mean slope is 17 %, but steep slopes (> 22 %) are common and occupy 28 % of the catchment, whereas gentle slopes (< 8 %) cover 22 % of the area (Fig. 1d).

The climate is Mediterranean continental type with mean annual rainfall of ca. 460 mm distributed in two rainy seasons, spring and autumn, and dry summers are characterized by frequent, high-intensity rainfall events (López-Vicente et al., 2008a). The mean annual temperature is 12.2ºC with common thermal inversions during the winter.

The study area is located at the transition between the Mediterranean and Sub Mediterranean bioclimatic regimes and the main vegetation cover consists of evergreen oak (*Quercus rotundifolia*) with some *Buxus sempervirens*, *Juniperus oxycedrus* and submediterranean plants, and the second dominant plant community dry-resistant deciduous oaks (*Quercus faginea* and *Quercus cerrioides*) with some *B. sempervirens*.

The long-term history of land use in the area has resulted in a patchwork of different land uses where natural vegetation is interspersed with cultivated land that is typical of Mediterranean agricultural landscapes. Farmland activities have been carried out since medieval times with agricultural and pasture uses. Intense anthropogenic activity has greatly modified landscapes in the catchment and has mainly affected the slope profiles by the construction of stone terraces for cereal crops and orchards. López-Vicente and Navas (2010) identified 17 different land uses.

A land use - land cover map was created by using GIS and a coloured orthophoto, and ten types of cover were identified for this study: cereal crops, dense and open Mediterranean forest (oak woodlands), scrublands, poplar and bank vegetation, pasture, paths and roads, bare soil, boulder and urban (Fig. 1c). The map provided the basis for calculating the area of each land use in the catchment by using ArcView GIS 3.2.

Winter barley is the main crop in the area (32 %) occupying the gentle slopes around the lakes in strong contrast with abrupt topography of steep slopes that are occupied by Mediterranean forests dense (23%) and open (21%), scrublands dense (9%) and sparse (8%) and riparian vegetation (3%) whereas almond and olive trees and pastures take up to <2% of the catchment. Bare soils and unpaved trail paths occupy around 3%.

2.2. *Digital elevation model and linear landscape elements*

To construct a reliable digital elevation model (DEM) of the study area the karstic nature and topographic complexity had to be considered. To this aim successive methodological approaches were used and further corrected in several field campaigns (López-Vicente and Navas, 2009; López-Vicente et al., 2011). A commercial grid DEM (5 x 5 m, cell size) was firstly used to derive a flow accumulation map of the area by

using the combined flow accumulation algorithm (MDD8) included in the HydroTools 1.0 extension (http://www.terracs.com/en/home.html). The DEM was corrected for flat areas (divides and vicinities of the lakes) by deriving contour lines at 3 m intervals. A coloured orthophoto (0.38 cm, cell size) was used for mapping the main topographic features and altitudinal data were measured on a regular grid (100 x 100 m) by using a Global Positioning System (GPS). Flat surfaces, gentle slopes and broad rounded ridges were characterized by measuring a number of elevation points with a Total Topographic Station (TTS). Then, the original contour lines were modified to obtain a new grid DEM from which a new flow accumulation map was obtained and an estimation of the error map was done by comparing the original and the new DEM. Finally, changes for forcing the directions of water courses were implemented after identification of the drainage system in the field. The detailed DEM and the analyses of the topographic features and of the characteristics of the hydrological network allowed the identification of a total of 9 endorheic sub-catchments and determination of the subcatchment that is the contributing area to the central lake (Fig. 1 b).

To accurately describe the soil redistribution of a catchment it is necessary to take into account the linear landscape elements (LLEs) that exist in the landscape (Vigiak et al., 2012). In the area LLEs were established following a long time of human intervention and previous research evidenced their important effect on the runoff pattern and, by extension, on sediment mobilization (López-Vicente et al., 2013). This has also been described in other recent works worldwide (e.g. Lesschen et al., 2009). There are a variety of man-made infrastructures and natural elements that modify the runoff pathways and thus the sediment connectivity (Callow and Smettem, 2009; Sougnez et al., 2011). In the catchment there are numerous LLEs and the distribution of the different types identified is: unpaved trails, drainage ditches, stone walls and barriers,

buffer strips and pond walls, vegetation strips and agricultural terraces, and other natural elements (scarps and boulders) (Fig. 1e).

2.3. *Soil and sediment sampling and analyses*

The predominant soil types in the catchment are stony Calcisols, Leptosols, Regosols and Gypsisols. Leptosols are restricted to the upper part of the slopes under Mediterranean forest, whereas Gypsisols cultivated for cereals occupy the lower parts (Machín et al., 2008).

The soils were sampled at the intersection points of an approximately 100 x 100 m grid totalling 154 samples providing ca. one soil sample per ha (Fig. 1b). The sampling grid was considered appropriate to represent the soil and physiographic diversity in the study area. An 8 cm diameter core driller was used to collect two replicates of bulk soil samples to the total depth of the soil profile. Under forest cover soil samples were collected from points located between the trees in open areas to avoid the effect of concentrated rainfall by stemflow. Gaspar et al. (2013) studied the vertical distribution of ^{137}Cs in the soils of the catchment and provided the basis to establish the depth of sampling depending on the soil type and land use. The studied ^{137}Cs depth profiles indicated that the first 15 cm contained 76-86% of the ^{137}Cs because the soils were undisturbed. For Leptosols the sampling depth was from 15 to 20 cm; therefore, it was assumed that the samples of Leptosols contained most of the total areal activity density of the soil at the sampling point. Sampling depth was 30 to 35 cm for Regosols. Deposition and cultivated sites on Calcisols and Gypsisols on the flat areas had longer profiles and therefore the sampling depth was extended above 50 cm to collect the entire ^{137}Cs profile.

Sediment accumulated on the lake shores was sampled at two sites using an 8 cm diameter core driller when the water level was low and the sediment of the littoral belt was exposed (Fig. 1b). In the lake shore cores the sedimentological facies were identified and correlated and depth interval subsamples were collected for gamma analyses. Chronological dating with ^{137}Cs was carried out on composite samples taken at same depth intervals.

Soil samples were stored at 4º C until analysed in the laboratory. Samples were air-dried, ground, homogenized, and quartered, before being passed through a 2-mm sieve. The coarse and fine-earth fractions were separated and weighted to account for the stoniness content (> 2 mm) and the total percentage of the < 2 mm fraction that fix the ^{137}Cs radionuclide (Quine et al., 1994). Radionuclide activity in the soil samples was measured at the gamma lab of the EEAD-CSIC using a high resolution, low background, low energy, hyperpure germanium, coaxial gamma-ray detector coupled to an amplifier and multichannel analyser (Canberra Xtra, Canberra industries, Inc. USA). The methods used in the gamma analysis are described in detail elsewhere (Navas et al., 2005). The detector is shielded to reduce background and has an efficiency of 30%, and 1.9 keV resolution at 1.33 MeV (^{60}Co). The detector was calibrated using certified samples in the same geometry and soil material as the measured samples. The gamma spectra were analysed using the Genie 2000 package (Canberra industries, Inc. USA). A total of 154 subsamples of 50 g were selected from the whole bulk soil samples and loaded into 125 cc cylindrical plastic containers. ^{137}Cs activity was determined from the 661.6 keV photopeak and its detection limit was 0.3 Bq kg^{-1}. Massic activities of ^{137}Cs were measured and results were decay-corrected to the sampling date. Replicates of 10 subsamples were tested to ensure repetitiveness of the results. Counting times were 30000 s and the analytical precision of the measurements was approximately ± 5%

(95% level of confidence). The content of ^{137}Cs in the soil sample is expressed as a concentration or massic activity (Bq kg^{-1} dry soil) and as activity per unit area or inventory (Bq m^{-2}), which is calculated using the weight of the < 2 mm fraction and the cross section of the core sampler.

General soil properties such as pH, electrical conductivity (EC), organic matter, carbonate, and gypsum contents were analysed according to standard procedures (CSIC, Consejo Superior de Investigaciones Científicas, 1976). Granulometric analyses were done to determine the soil texture. Contents of the clay, silt and sand fractions were measured using laser equipment. Samples were heated at 80º C with 10 % H_20_2 to eliminate the organic matter, chemically disaggregated with hexametaphosphate (40 %), stirred for 8 h and ultrasound was also used to facilitate particle dispersion. Soil organic matter (SOM) content was determined by the wet oxidation method using a titrimeter with a selective electrode.

Estimates of soil redistribution rates derived from ^{137}Cs measurements are based on a comparison of the total inventory for an individual sampling point and the local reference inventory (Walling and He, 1999). The reference inventory for the study area was 1570 ± 80 (s.d.) Bq m^{-2}. It was established from 9 ^{137}Cs sectioned profiles collected at stable reference sites (Navas et al., 2013). The reference sites were carefully selected to fulfil soil stability conditions where neither erosion nor deposition occurs. To this aim flat, undisturbed sites located at the divides of the subcatchments were selected and sampling was carried out in 2010. The ^{137}Cs profiles were consistent with those typically found at stable sites and the activity of ^{137}Cs decreased exponentially with depth (Fig. Supplemental Information (SI) 1). Where inventories are lower than the local reference inventory, loss of radionuclide points to loss of soil by erosion. Similarly,

inventories in excess of the reference level are indicative of addition of radionuclide and soil by deposition (Porto et al., 2013).

The models reported by Soto and Navas (2004 a, b; 2008) for uncultivated and cultivated soils have been applied to estimate soil redistribution rates. For uncultivated soils the model is compartmental and divides the soil into horizontal layers 1 cm thick with homogeneous ^{137}Cs distribution in each compartment and a time step of one month. A ^{137}Cs linear transference (Smith and Elder, 1999) between each pair of adjoining compartments is supposed, whereby the isotope flux is proportional to the difference in concentration between the two compartments, the proportionality constant being a specific coefficient k. In addition to the downward movement, the model also takes into account the ^{137}Cs deposition on the surface, which is known precisely in certain parts of the world (e.g. Blagoeva and Zikovsky, 1995). The increases or decreases in concentration level due to ^{137}Cs fluxes are corrected by a volume factor of the layers. This volume (V_f) is taken as the working volume for ^{137}Cs adsorption, which is considered to be the same as that occupied by the soil fraction less than 2 mm. The model considers the effective volume V_f to account for the stoniness, which in the Mediterranean soil environment is a main soil property.

Starting from a first monthly deposition on the soil surface

$$C(1, t) = C(1, t-1) + [d(t) / V_f(1)] \quad (1)$$

Where: C (1, t) is the ^{137}Cs concentration at the first compartment at time t; d (t) is the ^{137}Cs activity deposited at the soil surface, and $V_f(1)$ is the effective thickness of the first compartment. The program calculates F which is the ^{137}Cs flux towards the adjoining compartment and the consequent drop in concentration in the first compartment:

$$C(1, t) = C(1, t-1) + [d(t)/ V_f(1)] - [1/ V_f(1)] F [1 \rightarrow 2, t-1] \quad (2)$$

As in the first compartment, there exists in the remaining ones an entry flux, which increases the previous concentration and an exit flux, which reduces it. The program also calculates the radioisotope decay in the time interval being considered. The process is repeated for each time step, and each time includes deposition on the surface, the calculation of new concentrations in all compartments as a result of transfer between them, and the decrease in concentration as a result of radioactive decay.

Assuming that there is a constant rate of erosion the erosion rate is calculated according to equation (3).

$$C(z, t) = (1 / a(z)) [(a(z)- e) C(z, t) + e C(z +1, t)] \quad (3)$$

Where: a (z) is the thickness of the different layers; and e is the thickness lost each time step.

The ^{137}Cs loss term per surface unit in each compartment is calculated by multiplying the thickness e by the concentration of the compartment itself while the gain term is calculated by multiplying the thickness e by the concentration of the bottom compartment. The process of concentration calculation is repeated for every unit of time.

A second variable is added to quantify the deposition rate; the thickness of soil deposition, S (cm), modifying the concentration of ^{137}Cs in all layers according to equation (4):

$$C(z, t) = S C(z-1, t) + (1 - S) C(z, t) \quad (4)$$

For cultivated soils as the soil is mixed by tillage, the model has just one compartment that extends from the soil surface to a cultivation depth "H" (20 – 25 cm in the study area) and assumes a temporary evolution of the ^{137}Cs concentration in the compartment. The ^{137}Cs activity deposited is homogeneously distributed in the compartment within its V_f. Thus, if C (t) is the total inventory in a given t moment, c (t-1) is the total inventory

in the previous moment, and D (t) is the atmospheric ^{137}Cs deposition in that interval. Then, equation (5) is formulated as:

$$C(t) = C(t - 1) + D(t) \quad (5)$$

To estimate the decreases of ^{137}Cs inventories caused by erosion the model uses equation (6), where E is the thickness of the soil layer that is eroded per unit of time:

$$C(t) = C(t - 1)(1 - (E / H V_f) \quad (6)$$

Similarly, to estimate the increases of ^{137}Cs activity in the compartment for depositional sites, it uses equation (7), where F is the material deposited per unit of time. The model assumes that the deposited material comes from a short distance and has similar ^{137}Cs concentration than that of the analysed point.

$$C(t) = C(t - 1)(1 + (F / H V_f) \quad (7)$$

Potential errors and uncertainties (e.g. input of ^{137}Cs fallout at the study points, k values extracted from reference profiles and applied to undisturbed profiles are kept homogeneous in the profile) are propagated throughout the procedures for estimating soil redistribution rates and the uncertainty of the final estimates at the 95% level of confidence is ca. 10-15 %.

2.4. *Spatial analyses of ^{137}Cs, soil redistribution and sediment budget*

Considering the surface of the catchment, the total number of samples collected, and the representativeness of the land uses and physiographic characteristics of the study area we pondered whether or not the spatial distribution of ^{137}Cs data and estimates of redistribution rates could be approached by means of geospatial interpolation methods (cf. Di Stefano et al., 2005). To create the output maps of soil erosion and deposition from the input points of the converted values of ^{137}Cs inventories, we used ordinary kriging interpolation with a constant trend after examination of the average standard

errors for the 29 different kriging types assayed. Interpolation of non-measured data in a raster grid was done by using the weighted mean values of soil redistribution at the sampling points. Values were calculated on the basis of the distance between couples of points and the semi-variance of their values.

The maps of the isolevels of the soil redistribution rates were derived to represent their spatial distributions within the catchment. All maps, interpolations, and mathematical operations were performed using ArcView GIS© 3.2 and ArcMap™ 10.0.

In order to account for the effect of the man-made linear landscape elements (LLEs) on the processes of runoff accumulation and sediment trapping efficiency, and thus on the total sediment budget of the study area, a LLE mask was added. This mask modifies the soil loss and deposition maps obtained with kriging interpolation by adding values of soil loss for unpaved trails and values of soil deposition for the other LLEs. The new values correspond to the rates of soil loss and deposition measured at the closest sampling points to each LLE.

The sediment budget was established by computing the pixels on the map of soil redistribution rates, corresponding to different rates of soil loss and gain and deposition on the lake shores and the inner central lake. Deposition in the central lake was estimated from 4 short cores (0 - < 60 - 70 cm), two that were collected from the central part of the lake in a previous paleolimnological study (Morellón et al., 2011) and another two obtained on the lake shores. Chronological dating of the sediments with ^{137}Cs permitted to identify the 1963 ^{137}Cs peak. The thickness of the deposit was then converted into a mean annual deposition rate for the time span of the ^{137}Cs chronology.

Correlations were performed to analyse the relationships between ^{137}Cs and main soil properties. Analysis of variance was used to assess the significance of the effects of land

use and slope on the soil redistribution rates at the sampling points. Mean tests were carried out to confirm significant differences between the studied variables in terms of physiographic factors and land uses. Means that differed significantly ($p < 0.05$) were then determined using the Least Significant Difference (LSD Fisher) test.

3. **Results and discussion**

3.1. *Characteristics of the soils and of ^{137}Cs content distribution*

The soils of the Estanque Grande Catchment are alkaline with low electrical conductivity, low to moderate SOM contents, high carbonate contents and moderate gypsum contents except for the high percentages found in Gypsisols. The predominant textures are silty loams with high stoniness (Table SI 1).

The ^{137}Cs massic activities and inventories in the catchment soils ranged from 0.4 to 32.7 Bq kg^{-1} and 92 to 3869 Bq m^{-2}, respectively (Table SI 2) and fell within the range of values observed in the region and elsewhere in Spain (Navas et al., 2002, 2005, 2012, 2013). This relatively large variability has been observed in other catchments (e.g. Martinez et al., 2010, Kato et al., 2010).

The results of an ANOVA test detected significant differences between the radionuclide content in the soils under different land uses and land covers (Table SI 3), with lower massic activities in cultivated soils than in forest and scrubland soils. There were also significantly lower SOM and stoniness contents in cultivated soils in comparison to uncultivated ones, whereas the opposite was observed for values of bulk density, mass depth and profile depth. Differences in vegetation cover appear to be more related to differences in the main properties of the soils under different land uses. When examining whether differences in slope result in different ^{137}Cs massic activity

and inventory, SOM, stoniness and profile depth, it was found that high SOM and stone contents occur in soils on steep slopes that in turn are covered by forest or scrubland (Table 1). Thus, mean ^{137}Cs massic activities are higher and significantly different ($p \leq 0.05$) in soils on slopes with more than a 24º gradient compared to soils on slopes below 12º where the profile depth is significantly higher.

Correlations between the ^{137}Cs massic activities for the homogenized core and main soil properties were only significant for SOM and stoniness, although with the latter correlations were low ($r = 0.388$, $p \leq 0.01$). The ^{137}Cs massic activities were directly correlated with SOM contents ($r = 0.673$, $p \leq 0.01$). The radionuclide content tends to increase with an increase in SOM because the mobility of both ^{137}Cs and SOM is driven by the same processes. In addition, research on depth distribution of ^{137}Cs and SOM along a transect of the study area showed a great coincidence especially for undisturbed soils under forest (Gaspar and Navas, 2013) thus contributing to direct and significant relationships. This was further confirmed by the lower correlation found between ^{137}Cs and SOM in scrubland ($r = 0.345$, $p \leq 0.01$) compared to that in forests ($r = 0.713$, $p \leq 0.01$). Furthermore, the soils maintaining natural vegetation are better protected from erosion and in turn have high SOM and stoniness contents. This is supported by the significant, although low, correlations between ^{137}Cs and stoniness contents found in forests ($r = 0.370$, $p \leq 0.01$) compared to the lack of correlation in the rest of land covers and land uses.

In spite of ^{137}Cs being adsorbed onto clay surfaces or fixed within the lattice structure (e.g. Vanden Bygaart and Protz, 1995), correlations with clay percentages were not significant. The clay content in most samples was very homogeneous (about 22%) and this range of values did not contribute to producing strong correlations with ^{137}Cs. Furthermore, in undisturbed profiles of the study area Gaspar et al. (2013) found

the typical decay of ^{137}Cs massic activity with depth distribution whereas that of the clay content was homogeneous. Contrasting depth distributions could also contribute to the lack of significant correlations.

^{137}Cs massic activities exhibited a large spatial variability in the catchment (Fig. 2). The initial concentrations of the atmospherically-derived radionuclide depend on the spatial variability of its fallout. For large areas ^{137}Cs fallout is clearly dependent on rainfall, as it was found across an important altitudinal gradient in the central Ebro river basin (Navas et al., 2007). Spatial variations of ^{137}Cs fallout are also recorded for relatively small catchments with sea influence in Italy (Porto et al., 2009). This was not the case in the study catchment because the altitudinal gradient is small and rainfall does not vary. Other sources of variation, such as the Chernobyl accident (Higgitt et al., 1993; Golosov et al., 1999; Van der Perk et al., 2002) were negligible in our study area (Gaspar et al., 2013). Given that ^{137}Cs is rapidly adsorbed onto humic substances and the fine soil fraction (Kruyts and Delvaux, 2002), where it remains fixed in a very small number of sorbing sites, the main cause of its variation is likely to be related to its mobilization by physical processes. In spite of the fact that some ^{137}Cs vertical migration, mixing by bioturbation and plant uptake can occur (e.g. Schuller et al., 2002), water erosion and wind erosion trigger ^{137}Cs mobilization commonly associated with the fine soil fractions. Furthermore, in the study catchment an additional source of variation of ^{137}Cs derived from anthropogenic activity.

The highest ^{137}Cs massic activities were on the areas that maintained natural vegetation cover, both trees and scrubland, whereas the lowest values were found on cultivated fields (Fig. 2). This pattern is generally reported in different environments where higher percentages of vegetation cover are paralleled with high ^{137}Cs massic activities (Schoorl et al., 2004; Fukuyama et al. 2008, Navas et al., 2011).

In spite of physical processes of soil loss that might reduce the initial content of the radionuclide, the lowest ^{137}Cs massic activities were found in cultivated fields. This was expected because the mixing of the soil produced by tillage homogenizes the radionuclide content within the soil profile. Results of an ANOVA test of fixed factors that included land uses and SOM content codified in four levels (0-2, 2-4, 4-6 and >6%) indicated, with a 95% confidence level, that these two factors explained 68% of the variation of ^{137}Cs massic activities.

The reference inventory of 1570 ± 80 (s.d.) Bq m^{-2} established for the Estaña lakes catchment (Navas et al., 2013) was within the range for similar latitude - altitude locations in Spain (Navas et al., 2007). The spatial patterns of the ^{137}Cs inventories were only similar to those of ^{137}Cs massic activities in some of the forest areas close to the catchment divide, at the northern and south-western parts of the catchment (Fig. 2). The high ^{137}Cs inventories found in cultivated fields suggest intense mobilization of soil due to tillage practices. The significant differences in terms of the lower stone content of cultivated fields compared to forest areas indicate a relative enrichment of fine material by comparison to the forest soils thus contributing to increased ^{137}Cs inventories. The lowest values, which also occurred in cultivated fields and in degraded scrubland areas, reflected the complexity of the soil processes under different land uses.

The radionuclide loss and gain percentages that reflect soil erosion and soil deposition, respectively, are shown in Fig. 2 on the map of ^{137}Cs inventories. The magnitude and direction of the measured deviations from the local reference inventory provide a qualitative assessment of soil redistribution (Walling and He, 1999) and show a heterogeneous distribution, in accordance with the intricate landscape and the variety of land uses and land covers within the catchment.

3.2 *Spatial patterns of soil redistribution*

Estimates of erosion and deposition rates derived from ^{137}Cs measurements after conversion using appropriate models (Soto and Navas, 2004 a, b, 2008) show intense soil redistribution in the catchment (Fig. SI 2). Of the total 154 sampling points, 82 points (53 %) have experienced net soil loss whereas deposition is recorded in 50 points, in which soil gain has occurred over approximately the past 40- 50 years. At 22 sampling points negligible soil redistribution occurred as the values fall within the range of stability for the confidence interval around the mean value of the reference sites and thus are considered not to have experienced any net soil movement. The ranges of soil redistribution vary largely (Fig. SI 2), with erosion and deposition rates ranging between 0.1 and 140.5 Mg ha^{-1} yr^{-1} (CV: 163 %) and 0.1 and 82 Mg ha^{-1} yr^{-1} (CV: 159 %), respectively.

Soil redistribution rates (both erosion and deposition) lower than 0.9 Mg ha yr^{-1} predominated in areas covered by both dense and open forest, which maintain stable soil conditions (Fig. 3). The points that can be considered to be within the stability range were mainly located in the northern part of the catchment (7 points), but they were also found in the southern part (7 points), in areas with predominant scrubland vegetation. Other scattered points indicating stability were found under relicts of the natural forest and scrubland at the catchment divides (8 points).

A range of erosion rates from 1 to 10 Mg ha^{-1} yr^{-1} was found in areas of different slope gradients covered by natural vegetation of scrubland and forest (Fig. 3). Erosion rates above 40 Mg ha^{-1} yr^{-1} were recorded in crop fields mostly located in the northern part of the catchment on the south-facing slopes where soil loss reached as much as 140 Mg ha^{-1} yr^{-1} in a steep crop field. High rates of soil erosion were also found, although to

a lesser extent, in the southern part of the catchment where rates as high as 138.3 Mg ha^{-1} yr^{-1} were found mainly along the borders of cultivated fields due to tillage operations.

Points where soil deposition had taken place were relatively less abundant (32 %). Similarly to what was found for soil erosion, lower deposition rates predominated under forest and scrubland whereas higher deposition rates were mostly recorded in cultivated fields. A maximum of 82 Mg ha^{-1} yr^{-1} was recorded in a winter barley field on the lowland close to the lake, clearly associated with tillage.

The catchment presents strong topographic contrasts between the steep slopes that rise over the gentler ones surrounding the lakes. However, the highest soil redistribution rates for both erosion and deposition occurred on the gently sloping areas of the catchment. The means of erosion rates for the three slope intervals < 12º, 12º-24º and > 24º were 24.3, 18.9 and 15.3 Mg ha^{-1} yr^{-1}, respectively. In spite of the widely recognized effect of slope gradient on triggering erosion, there was a trend to lower rates for the higher slope gradients although differences were not statistically significant. For the same slope intervals the means of deposition rates, 17.7, 7.5 and 3.4 Mg ha^{-1} yr^{-1} respectively, were significantly higher on the gentler slopes compared to those on the steeper ones. In general, the steepest slopes are covered by shrubs and trees, and apart from few sloping fields of winter barley, most of the cultivated area spreads over the flat plains surrounding the lakes. These results point to the fact that the most intense soil redistribution in the study catchment is related to cultivation of the land and that tillage induced both erosion and deposition.

An ANOVA test of fixed factors that included land uses and SOM content codified in four levels (0-2, 2-4, 4-6 and >6%) established, with a 95% confidence level, that two factors explained 43 % and 50 % of the variation of erosion and deposition rates,

respectively. Land use and land cover had a significant effect on the soil redistribution rates. In forest and scrubland the median erosion rates ranged from 3.2 to 6.0 Mg ha^{-1} yr^{-1} while the medians of soil deposition were lower (1.5 to 2.1 Mg ha^{-1} yr^{-1}). Tillage practices are responsible for higher rates of soil redistribution on the relatively gentle slopes occupied by farmland in this mountain catchment. Median estimates of both soil erosion and deposition in fields of cereal crops amounted to as much as 23.4 Mg ha^{-1} yr^{-1} and 20.4 Mg ha^{-1} yr^{-1}, respectively. Similar results were found in nearby temperate areas (Navas et al., 2005), as well as in previous research in the adjoining catchment (Gaspar et al., 2013, Navas et al., 2013).

Furthermore, simulated soil erosion data for the whole catchment of the Estaña lakes (2.4 km^2) obtained by applying semi-physical-based models, provided average rates that were comparable to those derived from the ^{137}Cs estimates. Thus, simulation with the RMMF (Revised Morgan, Morgan and Finney) and SEDD (Sediment Delivery Distributed) models estimated an average erosion rate in the whole catchment of 11.9 Mg ha^{-1} yr^{-1}, reaching 170.3 Mg ha^{-1} yr^{-1} within a raster cell in a steep gully (López-Vicente and Navas, 2010 a, b). However, the RUSLE (Revised Universal Soil Loss Equation) model estimated an average soil loss of 2.3 Mg ha^{-1} yr^{-1} (López-Vicente and Navas, 2009). These figures suggest that rates under forest and scrubland might be underestimated because RUSLE is an empirical model designed for cultivated land. However, the highest rates simulated with RUSLE on steep cultivated fields were 30% higher than the ^{137}Cs rates.

Means of erosion rates were 5 to 12 times higher and significantly different in winter barley fields than in the rest of the land covers (Table 2). The key role of cultivation as main driver of soil erosion has been recognized in a variety of environments, from temperate to semiarid (e.g. Mabit et al., 2002, Navas and Walling, 1992; Quine et al.,

1994). Under scrubland the erosion rates were lower and less variable than under forest, suggesting the highly protective effect of scrub vegetation in Mediterranean environments. With regard to deposition rates a similar pattern is observed with mean values that were 8 times higher in cultivated fields than in the rest of land covers which present fairly moderate deposition rates.

The highly heterogeneous patterns of spatial soil redistribution reflected the complexity of the intricate mosaic of land uses and land covers in an area of steep terrain.

3.3 Sediment budget

The spatial distribution of erosion and deposition rates estimated from the ^{137}Cs measurements provides a framework for establishing a sediment budget in the catchment which is a key issue in assessing siltation rates of the mountain wetland that has experienced a rapid retreat over the last few decades. Furthermore, catchment sediment budgets provide an improved understanding of catchment functioning and are of great value for designing effective sediment management strategies (Walling and Collins, 2008).

The converted values of soil erosion and deposition from the ^{137}Cs measurements were used directly for a kriging interpolation procedure that was based in the semi-variogram presented in Fig. 4. The kriging map of soil redistribution was used as the basis for estimating the percentage distribution of the areas experiencing soil loss or accumulation in the study area after computing erosion and deposition data from each pixel (5 x 5 m resolution). The percentage of eroded surfaces for the whole catchment

amounted to 55 %, exceeding that of depositional areas, including lake surfaces and the littoral vegetation belt (43 %).

For the 1.05 Km^2 subcatchment that directly supplies sediment to the central lake, i.e. the contributing catchment (Fig. 4), the eroding areas (63 %) also exceeded the depositional ones (35 %) and consequently a substantial sediment load is expected to be transported to the lake. Inclusion of the LLEs (Fig. 1e) that interrupt the connectivity of runoff reduced the eroding areas (0.9 %) and increased the depositional ones (1.0 %) affecting the estimates of soil redistribution and sediment yield exported to the lake. Taking into account the LLEs identified in eroding areas that amounted to 18550 m^2 the total soil loss was reduced from 1103 to 1068 Mg yr^{-1} and average soil erosion decreased from 16.6 to 16.2 Mg ha^{-1} yr^{-1}. When computing the LLEs in depositional areas, which extended over 16650 m^2, total soil deposition increased from 383 to 397 Mg yr^{-1} and the average soil deposition increased slightly from 10.5 to 10.7 Mg ha^{-1} yr^{-1}. Similar effects were obtained after simulation of different land cover management practices in a temperate Pyrenean catchment (López-Vicente et al., 2011). On average, for the time span of the ^{137}Cs estimates, a net soil loss of 671 Mg yr^{-1} is estimated after subtracting from the total soil erosion, the total soil deposition in the contributing catchment, which considering its total surface amounts to 6.39 Mg ha^{-1} yr^{-1}.

A multi-proxy study by Morellón et al. (2011) reconstructed the main phases of environmental change for an 860-year sequence in the Estaña Lake and found a gradual increase of farming activity from 1300 to 1850 AD. The absolute radioisotopic chronology (AMS radiocarbon dating and ^{210}Pb and ^{137}Cs) revealed that intense farming occurred at the end of the 19th century coinciding with maximum lake levels. This was followed by a decline in agriculture causing land abandonment during the mid-nineteen

fifties at the same time that a decline in lake levels occurred, associated with a warmer climate during the 20th century.

Taking the deposited sediment in the lake into account, the 15 cm deep ^{137}Cs peak in the inner lake core (Morellón et al., 2011) represents an average deposit of 0.375 cm yr^{-1}. On the lake shore cores the ^{137}Cs peak found at 45 cm depth represents a higher accumulation at a rate of 1.125 cm yr^{-1} due to the trapping of sediments by the littoral vegetation (Fig. 4). The predominant high rates of erosion by water and tillage recorded at the sampling points on the cultivated fields surrounding the lake support a direct source of sediment supply to the central lake.

The ^{137}Cs peaks found in the sediment cores of the inner lake and the lake shores indicated that sediment has accumulated at a rate of 45.8 and 113.2 Mg ha^{-1} yr^{-1}, respectively. Considering the bulk density of the sediments (1.22 g cm^{-3}), the average mass load accumulated in the central lake could amount to ca. 25560 Mg. Therefore, the rate of sediment accumulation over the last half century had almost doubled that which occurred over 860 years (Morellón et al., 2011). Widespread mechanization of farming activities in the last part of the 20th century seems to be a key control factor of the recent intensification of erosion in the catchment.

From these records, the sediment accumulated in the lake at a rate of 639 Mg yr^{-1}, results in a specific sediment yield from the contributing area of 6.20 Mg ha^{-1} yr^{-1}. For the riparian littoral belt surrounding the lake an average sedimentation rate of 38.3 Mg ha^{-1} yr^{-1} was recorded from the core data and from bulk samples at 5 points located around the lake, after calculating the relative contribution of their respective surfaces (Fig. 4). The sediment trapped by the riparian littoral vegetation on the lake shores that extends over 36400 m^2 is less than that accumulated in the central lake (151900 m^2). In total, considering both the sediment deposits in the lake and the lake shores that

accumulated at a rate of 139 Mg yr^{-1} (1.36 Mg ha^{-1} yr^{-1}), the specific sediment yield amounts to 7.56 Mg ha^{-1} yr^{-1}.

Sediment accumulated in the lake and trapped in the riparian vegetation belt was generated both from interrill/rill erosion and gully erosion. From the ^{137}Cs data a net soil loss of 671 Mg yr^{-1} ca. to 6.39 Mg ha^{-1} yr^{-1} was estimated after subtracting total soil deposition in the contributing catchment from total soil erosion. Since ^{137}Cs only accounts for interrill/rill erosion, the rest of the sediment supply (ca. 1.16 Mg ha^{-1} yr^{-1}) can be attributed to gully erosion. This lower contribution from gullies than from interrill erosion appears to be consistent with the specific features of the gullies in the study area that occupy only 17300 m^2, and as can be seen in Fig. 1 b, do not inflow directly into the lake.

The schematic representation of the sediment budget in Fig. 5 depicts the distribution of the amount of soil erosion and deposition related to the different land uses and hydrologic compartments, such as gullies and ephemeral gullies and the lake in the study catchment. In accordance with its endorheic character sediment is stored within the catchment and deposited mainly in the central lake and the lake shores. Deposition is also important in other compartments of the catchment, especially on slopes occupied by cultivated fields. Evidence of the importance of sediment intrastorage within river catchments has also been demonstrated by Porto et al. (2013) in the Italian Bonis catchment where deposition occurring on slopes and the channel system results in low sediment delivery ratios.

Human intervention on the landscapes of the Estaña lakes and land management carried out in the area to preserve the agricultural soils may explain why the gullies stop prior to reaching the agricultural fields of the lowlands. Thus, the agricultural fields function as a buffer area around the lakes and the sediments transported in the gullies

might only reach the lake directly during intense storm events. Evidence of this was found in the inner lake core, where a peak of carbonates found in its upper part (Morellón et al., 2011) could be related to the frequent storm events that occurred in the area around the mid-nineteen eighties (Beguería et al., 2011). However, the agricultural fields surrounding the lake directly supply sediments to the lake from water and tillage erosion as no conservation measures are carried out to preserve the wetlands. This results in eroded materials from agricultural fields directly reaching the inner parts of the lake. The other sediment portion is trapped in the riparian vegetation of the littoral belt evidence of which is provided by the 45 cm sediments accumulated in the lake shore core.

4. Conclusions

Application of a ^{137}Cs method that measures soil redistribution, and thus accounts for both soil erosion and soil deposition, enabled us to derive estimates of soil redistribution rates and establish a sediment budget at the catchment scale. The methods used allow for identifying the main factors triggering erosion and the sources of sediment, which is a basic requirement for assessing the risk of wetland siltation with the aim of conserving endangered wetlands.

The spatial distribution of the soil erosion and deposition rates indicates that higher soil redistribution occurs in the lowlands with predominant agricultural use. Lower rates of soil erosion on steeper slopes can be explained by the vegetation cover. Therefore, land use and distribution of vegetation cover are the main controlling factors of soil redistribution. Mediterranean dense and open forests occupying the highlands, interspersed with scrublands on high to moderate slopes efficiently protect the soil

surface from erosion. Croplands occupying more gentle slopes and lowlands exhibit the greatest rates of soil loss and soil deposition due to cultivation under traditional tillage practices.

The karstic nature of this catchment compounded the difficulty of the soil redistribution estimates, but the high spatial resolution of the corrected DEM within a GIS basis provided a framework for identifying the part of the catchment that was supplying sediment to the lake in this complex landscape. With this mehtod we could discriminate and separate a total of 8 small subcatchments that were not directly contributing to the siltation of the central lake included in the European NATURA 2000 Network as a Site of Community Importance.

The data set generated from ^{137}Cs estimates suggests that interrill erosion by water and tillage is more prominent than gully erosion. Evidence of human intervention modified the original landscapes by creating numerous linear landscape elements that disconnected runoff and interrupted the gullies reaching the lake thus limiting the sediment supply from this source. However, sediment by water and tillage erosion from the agricultural fields surrounding the lake contributes substantially to the current lake siltation. Mechanization of agricultural practices in the last part of the 20^{th} century also has led to increase rates of lake siltation. To protect wetlands the introduction of strips of vegetation at the lower end of the fields would be a protective measure that could be implemented for the preservation of this endangered wetland area.

The results outline the value of combining radiotracing and GIS techniques to obtain comprehensive information on the sources and sinks of sediment and the factors that affect its redistribution in agricultural upland landscapes. Information obtained here can be used for implementing soil conservation procedures and sediment controls to reduce

sediment loads and avoid siltation and contamination of water bodies, particularly fragile mountain wetlands.

Acknowledgements

We thank the CICYT project EROMED (CGL2011-25486) for the financial support.

References

Beguería S, Angulo-Martínez M, Vicente-Serrano SM, López-Moreno JI, Kenawy A. Assessing temporal trends in extreme precipitation by non-stationary peaks-over-threshold analysis, NE Spain 1930-2006. Int J Climatol 2011;31:102-2114.

Blagoeva R, Zikovsky L. Geographic and vertical distribution of Cs-137 in soils in Canada. J Environ Radioactiv 1995;27:269-274.

Borselli L, Cassi P, Torri D. Prolegomena to sediment and flow connectivity in the landscape: A GIS and field numerical assessment. Catena 2008;75:268–277.

Callow JN, Smettem KRJ. The effect of farm dams and constructed banks on hydrologic connectivity and runoff estimation in agricultural landscapes. Environ Modell Softw 2009;24:959–968.

Cerdà A. Soil erosion after land abandonment in a semiarid environment of southeastern Spain. Arid Soil Res Rehab 1997;11(2):163–176.

CSIC, Consejo Superior de Investigaciones Científicas. Comisión de métodos analíticos. An Edaf Agrobiol 1976;35:813-814.

Di Stefano C, Ferro V, Porto P, Rizzo S. Testing a spatially distributed sediment delivery model (SEDD) in a forested basin by caesium-137 technique. J Soil Water Conserv 2005;60(3):148-157.

Everard M. Investing in sustainable catchments. Sci Total Environ 2004;324:1–24.

Fukuyama T, Onda Y, Takenaka C, Walling DE. Investigating erosion rates within a Japanese cypress plantation using Cs-137 and Pb-210ex measurements. J Geophys Res 2008;113, art. no. F02007.

García-Ruiz JM. The effects of land uses on soil erosion in Spain: A review. Catena 2010;81(1):1–11.

Gaspar L, Navas A. Vertical and lateral distributions of ^{137}Cs in cultivated and uncultivated soils on Mediterranean hillslopes. Geoderma 2013;207-208:131-143.

Gaspar L, Navas A, Walling DE, Machín J, Gómez Arozamena J. Using ^{137}Cs and $^{210}Pb_{ex}$ to assess soil redistribution on slopes at different temporal scales. Catena 2013;102:46-54.

Golosov VN, Walling DE, Panin AV, Stukin ED, Kvasnikova EV, Ivanova NN. The spatial variability of Chernobyl-derived ^{137}Cs inventories in a small agricultural draiange basin in central Russia. Appl Radiat Isotopes 1999;51:341-352.

Higgitt DL, Rowan JS, Walling DE. Catchment-scale deposition and redistribution of Chernobyl radiocaesium in upland Britain. Environ Int 1993;19:155-166.

IAEA, 1990. Environmental Isotope Data No. 9: World Survey of Isotope Concentration in Precipitation (1984-1987). Tech Reports Series 1990; 311.

IGME. Mapa Geológico de España 1:50.000. No. 289: Benabarre. Instituto Geológico y Minero de España, Madrid. 1982.

Kato H, Onda Y, Tanaka H. Using ^{137}Cs and $^{210}Pb_{ex}$ measurements to estimate soil redistribution rates on semi-arid grassland in Mongolia. Geomorphology 2010;114: 508–519.

Kruyts N, Delvaux B. Soil organic horizons as a major source for radiocesium biorecycling in forest ecosystems. J Environ Radioactiv 2002;58 (2-3):175-190.

Lesschen JP, Schoor JM, Cammeraat LH. Modelling runoff and erosion for a semi-arid catchment using a multi-scale approach based on hydrological connectivity. Geomorphology 2009;109(3-4):174–183.

López-Vicente M, Navas A, Machín J. Identifying erosive periods by using RUSLE factors in mountain fields of the Central Spanish Pyrenees. Hydrol Earth Syst Sc 2008a;12:523–535.

López-Vicente M, Navas A, Machín J. Modelling soil detachment rates in rainfed agrosystems in the south-central Pyrenees. Agr Water Manage 2008b;95(9):1079-1089.

López-Vicente M, Navas A. Predicting soil erosion with RUSLE in Mediterranean agricultural systems at catchment scale. Soil Sci 2009;174(5):272–282.

López-Vicente M, Navas A. Relating soil erosion and sediment yield to geomorphic features and erosion processes at the catchment scale in the Spanish Pre-Pyrenees. Environ Earth Sci 2010a;61(1):143–158.

López-Vicente M, Navas A. Routing runoff and soil particles in a distributed model with GIS: implications for soil protection in mountain agricultural landscapes. Land Degrad Dev 2010b;21(2):100-109.

López-Vicente M, Lana-Renault N, García-Ruiz JM, Navas A. Assessing the potential effect of different land cover management practices on sediment yield from an abandoned farmland catchment in the Spanish Pyrenees. J Soil Sediment 2011;1(8):1440–1455.

López-Vicente M, Poesen J, Navas A, Gaspar L. Predicting runoff and sediment connectivity and soil erosion by water for different land use scenarios in the Spanish Pre-Pyrenees. Catena 2013;102:62–73.

Mabit L, Bernard C, Laverdière MR. Quantification of soil redistribution and sediment budget in a Canadian watershed from fallout caesium-137 (^{137}Cs) data. Can J Soil Sci 2002;82:423-431.

Mabit L, Bernard C. Assessment of spatial distribution of fallout radionuclides through geostatistics concept. J Environ Radioactiv 2007;97:206-219.

Mabit L, Bernard C, Laverdière MR. Spatial variability of erosion and soil organic matter content estimated from ^{137}Cs measurements and geostatistics. Geoderma 2008;145:245-251.

Machín J, Navas A. Spatial analysis of gypsiferous soils in the Zaragoza province (Spain), using GIS as an aid to conservation. Geoderma 1998;87:57-66.

Machín J, López Vicente M, Navas A. Cartografía digital de suelos de la Cuenca de Estaña (Prepirineo Central). En: Benavente J, Gracia FJ, ed. Trabajos de Geomorfología en España. 2006-2008. SEG; 2008. pp.481-484.

Manen C, Sabatier P. Chronique radiocarbone de la néolithisation en Méditerranée bord-occidentale**.** B Soc Préhist Fr 2003;100(3): 479-504.

Martinez C, Hancock GR, Kalma, JD. Relationships between ^{137}Cs and soil organic carbon (SOC) in cultivated and never-cultivated soils: An Australian example. Geoderma 2010;158:137-147.

Morellón M, Valero-Garcés BL, González-Sampériz P, Vegas-Vilarrúbia T, Rubio E, Rieradevall M, Delgado-Huertas A, Mata P, Romero O, Engstrom DR, López-Vicente M, Navas A, Soto J. Climate changes and human activities recorded in the sediments of Lake Estanya (NE Spain) during the Medieval Warm Period and Little Ice Age. J Paleolimnol 2011;46(3):423-452.

Navas A, Walling D. Using caesium-137 to assess sediment movement in a semiarid upland environment in Spain. In: Walling DE, Davies TR, Hasholt B, editors. Erosion, Debris Flows and Environment in Mountain Regions. IAHS Publ. 1992;209:129-138.

Navas A, Soto J, Machín J. ^{238}U, ^{226}Ra, ^{210}Pb, ^{232}Th and ^{40}K activities in soil profiles of the Flysch sector (Central Spanish Pyrenees). Appl Radiat Isotopes 2002;57(4):579-589.

Navas A, Machín J, Soto J. Assessing soil erosion in a Pyrenean mountain catchment using GIS and fallout ^{137}Cs. Agr Ecosyst Environ 2005;105: 493-506.

Navas A, Walling DE, Quine T, Machín J, Soto J, Domenech S, López-Vicente M,. Variability in ^{137}Cs inventories and potential climatic and lithological controls in central Ebro valley, Spain. J Radioan Nucl Chem 2007;274:331-339.

Navas A, Gaspar L, López-Vicente M, Machín J. Spatial distribution of natural and artificial radionuclides at the catchment scale (South Central Pyrenees). Radiat Meas 2011;46(2):261-269.

Navas A, Gaspar L, Quijano L, López-Vicente M, Machín J. Patterns of soil organic carbon and nitrogen in relation to soil movement under different land uses in mountain fields (South Central Pyrenees). Catena 2012;94:43-52.

Navas A, López-Vicente M, Gaspar L, Machín J. Assessing soil redistribution in a complex karst catchment using fallout ^{137}Cs and GIS. Geomorphology 2013;196: 231–241.

Porto P, Walling DE, Ferro V, Di Stefano C. Validating erosion rate estimates provided by caesium-137 measurements for two small forested catchments in Calabria, Southern Italy. Land Degrad Dev 2003;14:389-408.

Porto P, Walling DE, Callegari G, Capra A. Using caesium-137 and unsupported lead-210 measurements to explore the relationship between sediment mobilization, sediment delivery and sediment yield for a Calabrian catchment. Mar Freshwater Res 2009;60:680-689.

Porto P, Walling DE, Callegari G. Using ^{137}Cs measurements to establish catchment sediment budgets and explore scale effects. Hydrol Process 2011;25:886-900.

Porto P, Walling DE, Callegari G. Using ^{137}Cs and ^{210}Pbex measurements to investigate the sediment budget of a small forested catchment in southern Italy. Hydrol Process 2013;27:795-806.

Quine T, Navas A, Walling DE, Machín J. Soil erosion and redistribution on cultivated and uncultivated land near Las Bardenas in the Central Ebro River Basin, Spain. Land Degrad Rehabil 1994;5:41–55.

Ritchie JC, McCarty GW. Redistribution of soil and soil organic carbon on agricultural landscapes. Sediment Dynamics in Changing Environments. (Proceedings of a symposium held in Christchurch, New Zealand); 2008. IAHS Publ. 325:135-138.

Ruiz-Navarro A, Barberá GG, García-Haro J, Albaladejo J. Effect of the spatial resolution on landscape control of soil fertility in a semiarid area. J Soil Sedimen. 2012;12(4):471-485.

Schoorl JM, Boix Fayos C, de Meijer RJ, van der Graaf ER, Veldkamp A. The Cs-137 technique applied to steep Mediterranean slopes (Part I): the effects of lithology, slope morphology and land use. Catena 2004;57:15-34.

Schuller P, Voigt G, Handl J, Ellies A, Oliva L. Global weapons' fallout ^{137}Cs in soils and transfer to vegetation in south-central Chile. J Environ Radioactiv 2002;62:181-193.

Smith JT, Elder DG. A comparison of models for characterizing the distribution of radionuclides with depth in soils. Eur J Soil Sci 1999;50:295-307.

Soto J, Navas A. A model of ^{137}Cs activity profile for soil erosion studies in uncultivated soils of Mediterranean environments. J Arid Environ 2004a;59:719-730.

Soto J, Navas A. Modelo de simulación del perfil de cesio-137 para cuantificar el depósito de suelo. Geo-Temas 2004b;6:273-275.

Soto J, Navas A. A simple model of ^{137}Cs profile to estimate soil redistribution in cultivated stony soils. Radiat Meas 2008;43:1285-1293.

Sougnez N, van Wesemael B, Vanacker V. Low erosion rates measured for steep, sparsely vegetated catchments in southeast Spain. Catena 2011;84(1-2):1–11.

Staunton S, Dumat C, Zsolnay A. Possible role of organic matter in radiocaesium adsorption in soils. J Environ Radioactiv 2002;58:163-173.

Tamura T. Selective sorption reactions of caesium with mineral soils. Nucl Safety 1964; 5:263-268.

Valero-Garcés B, González-Sampériz P, Navas A, Machín J, Mata P, Delgado-Huertas A, Bao R, Moreno Caballud A, Carrión J, Schwalb A, González-Barrios A. Human impact since medieval times and recent ecological restoration in a Mediterranean Lake: The Laguna Zoñar, southern Spain. J Paleolimnol 2006; 35: 441-465

Van der Perk M, Stavik O, Futajtár E. Assessment of spatial variation of cesium-137 in small catchments. J Environ Qual 2002;31:1930-1939.

Vanden Bygaart AJ, Protz R. Gamma radioactivity on a chronosequence, Pinery Provincial Park, Ontario. Can J Soil Sci 1995;75:73-84.

Vigiak O, Borselli L, Newham LTH, McInnes J, Roberts AM. Comparison of conceptual landscape metrics to define hillslope-scale sediment delivery ratio. Geomorphology 2012;138:74–88.

Walling DE, Collins AL. The catchment sediment budget as a management tool. Environ Sci Policy 2008;11(2):136-143.

Walling DE, He Q. Improved models for estimating soil erosion rates from cesium-137 measurements. J Environ Qual 1999;28:611-622.

Walling DE, Collins AL, Jones PA, Leeks GJL, Old G. Establishing fine-grained sediment budgets for the Pang and Lambourn LOCAR catchments, UK. J Hydrol 2006;330:126-141.

Figures

Figure 1.- The study area in the central part of the Ebro basin in the Southern Pyrenean border. a) ArcScene of the Estanque Grande Catchment; b) Digital elevation model of the study area, location of the sampling points and the reference sites, the subcatchment divides, and the systems of gullies; c) Land use and land cover map; d) Map of the slope gradients; e) Location of the 9 different types of landscape linear elements identified in the Estanque Grande catchment.

Figure 2 .- Spatial distribution of ^{137}Cs massic activities and inventories and of the radionuclide loss and gain percentages in the Estanque Grande catchment.

Figure 3.- Rates of soil erosion and deposition (Mg ha^{-1} yr^{-1}) in the sampling points of the study area.

Figure 4.- Map of the spatial distribution of the soil erosion and deposition rates in the subcatchment directly supplying to the Estanque Grande used to establish the sediment budget. Massic activity of ^{137}Cs in the lake shore cores and depth of the 1963 ^{137}Cs peak. * Depth at which the 1963 ^{137}Cs peak was identified in the inner lake core (Morellón et al., 2011). Semivariogram of the ^{137}Cs converted data used for the kriging interpolation of the soil redistribution rates.

Figure 5.- Schematic representation of the sediment budget and distribution of the amount of soil erosion and deposition related to the different land uses/land covers and hydrologic compartments in the study catchment.

Table 1. Least square mean concentrations of ^{137}Cs massic activities and inventories, SOM and stoniness contents and profile depth for the different slope gradients in the catchment and the percentage distribution of land uses for each slope range.

						^{137}Cs		^{137}Cs		SOM		Stoniness		Profile depth	
						Bq kg^{-1}		Bq m^{-2}		%		%		cm	
		Land uses %													
	n	DF	OF	S	WB										
0 - 12%	51	12	10	16	62	7.4	a	1675.1	b	3.0	a	25.0	a	35	a
12 - 24%	77	28	25	19	28	10.0	ab	1330.4	a	4.4	b	29.6	a	25	a
> 24%	26	34	33	20	13	11.8	b	1467.9	ab	4.2	ab	29.6	a	23	b

Different letters indicate significant differences at the p-level < 0.05
Land uses: *DF: Dense Mediterranean Forest, OF: Open Mediterranean forest, S: Scrubland, WB: Winter Barley*

Table 2. Basic statistics of soil erosion and deposition rates (Mg ha^{-1} $year^{-1}$) in the soils of the catchment under the different uses and land covers.

Mg ha^{-1} $year^{-1}$	n	Mean		SD	SE	CV %	Min.	Max.
Erosion rate								
Dense Med Forest	20	5.8	a	9.5	2.1	163.9	0.1	42.4
Open Med Forest	15	7.9	a	8.6	2.2	109.3	0.4	32.8
Scrubland	20	3.6	a	4.2	0.9	115.2	0.2	19.2
Winter Barley	33	43.5	b	42.3	7.4	97.3	2.6	140.5
total	88	19.8		32.2	3.4	162.7	0.1	140.5
Deposition rate								
Dense Med Forest	12	3.0	a	3.5	1.0	117.6	0.1	11.6
Open Med Forest	18	2.9	a	2.9	0.7	99.4	0.1	9.0
Scrubland	13	3.2	a	3.6	1.0	111.4	0.3	13.5
Winter Barley	23	25.8	b	22.7	4.7	88.2	0.7	82.0
total	66	10.9		17.3	2.1	158.5	0.1	82.0

SD standard deviation
SE standard error
CV coefficient of variation

Different letters indicate significant differences at the p-level < 0.05

Fig. 1

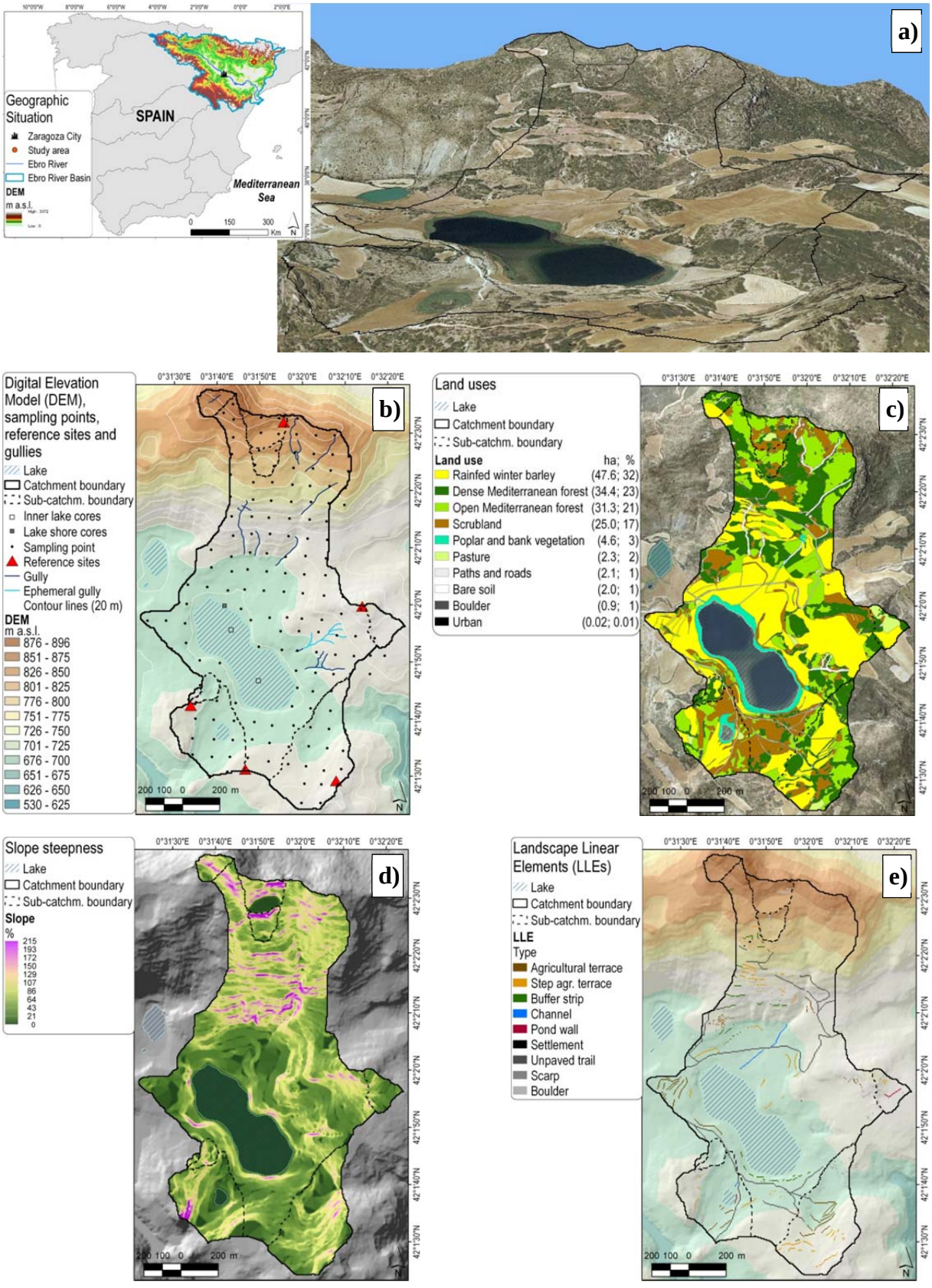
Geographic Situation
Zaragoza City
Study area
Ebro River
Ebro River Basin
DEM
m a.s.l.
SPAIN
Mediterranean Sea
0 150 300 Km
a)
Digital Elevation Model (DEM), sampling points, reference sites and gullies
Lake
Catchment boundary
Sub-catchm. boundary
Inner lake cores
Lake shore cores
Sampling point
Reference sites
Gully
Ephemeral gully
Contour lines (20 m)
DEM
m a.s.l.
876 - 896
851 - 875
826 - 850
801 - 825
776 - 800
751 - 775
726 - 750
701 - 725
676 - 700
651 - 675
626 - 650
530 - 625
b)
Land uses
Lake
Catchment boundary
Sub-catchm. boundary
Land use ha; %
Rainfed winter barley (47.6; 32)
Dense Mediterranean forest (34.4; 23)
Open Mediterranean forest (31.3; 21)
Scrubland (25.0; 17)
Poplar and bank vegetation (4.6; 3)
Pasture (2.3; 2)
Paths and roads (2.1; 1)
Bare soil (2.0; 1)
Boulder (0.9; 1)
Urban (0.02; 0.01)
c)
Slope steepness
Lake
Catchment boundary
Sub-catchm. boundary
Slope
%
215
193
172
150
129
107
86
64
43
21
0
d)
Landscape Linear Elements (LLEs)
Lake
Catchment boundary
Sub-catchm. boundary
LLE
Type
Agricultural terrace
Step agr. terrace
Buffer strip
Channel
Pond wall
Settlement
Unpaved trail
Scarp
Boulder
e)
200 100 0 200 m
N

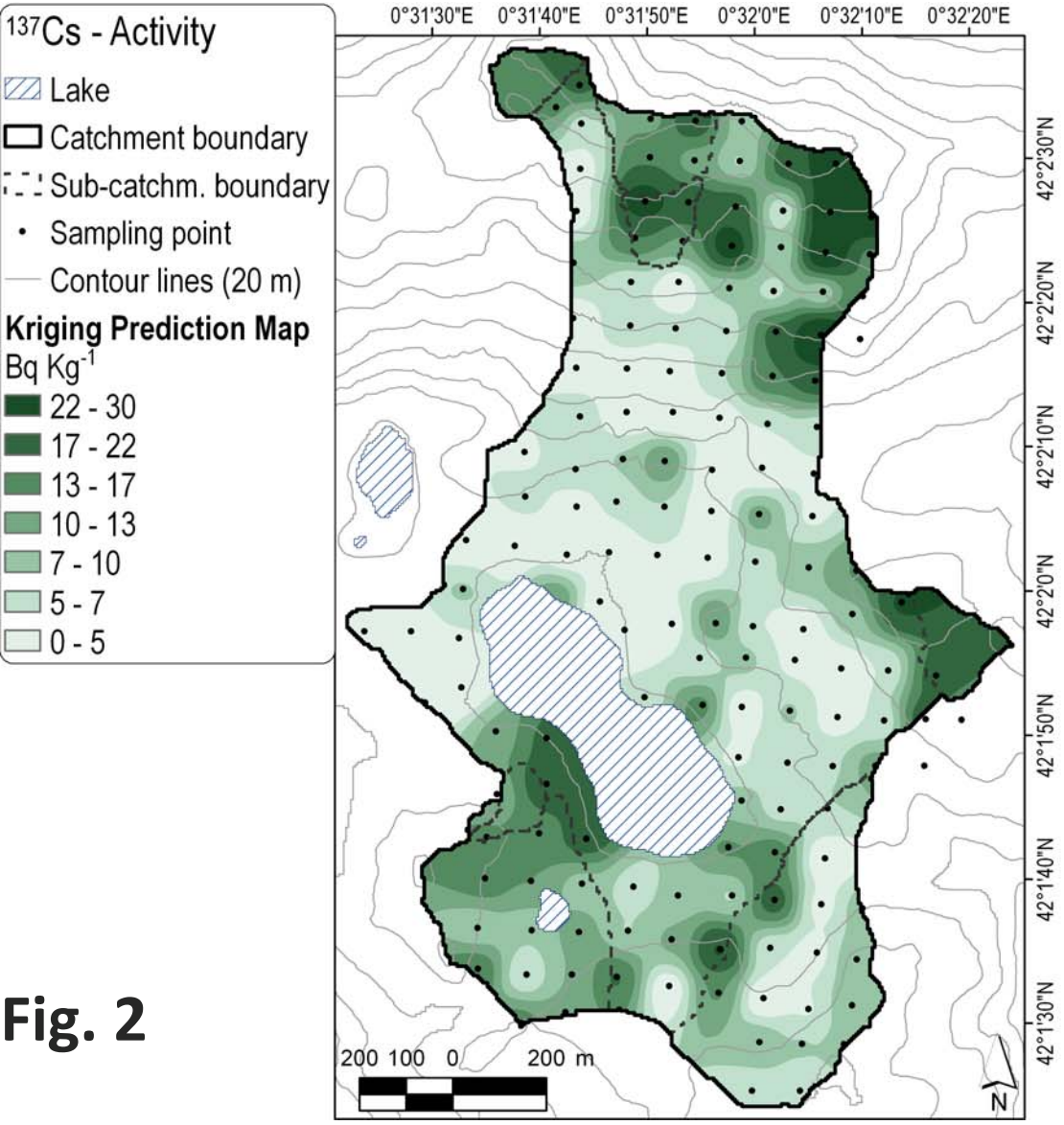
137Cs - Activity
Lake
Catchment boundary
Sub-catchm. boundary
Sampling point
Contour lines (20 m)
Kriging Prediction Map
Bq Kg-1
22 - 30
17 - 22
13 - 17
10 - 13
7 - 10
5 - 7
0 - 5
0°31'30"E
0°31'40"E
0°31'50"E
0°32'0"E
0°32'10"E
0°32'20"E
42°2'30"N
42°2'20"N
42°2'10"N
42°2'0"N
42°1'50"N
42°1'40"N
42°1'30"N
200 100 0 200 m
N

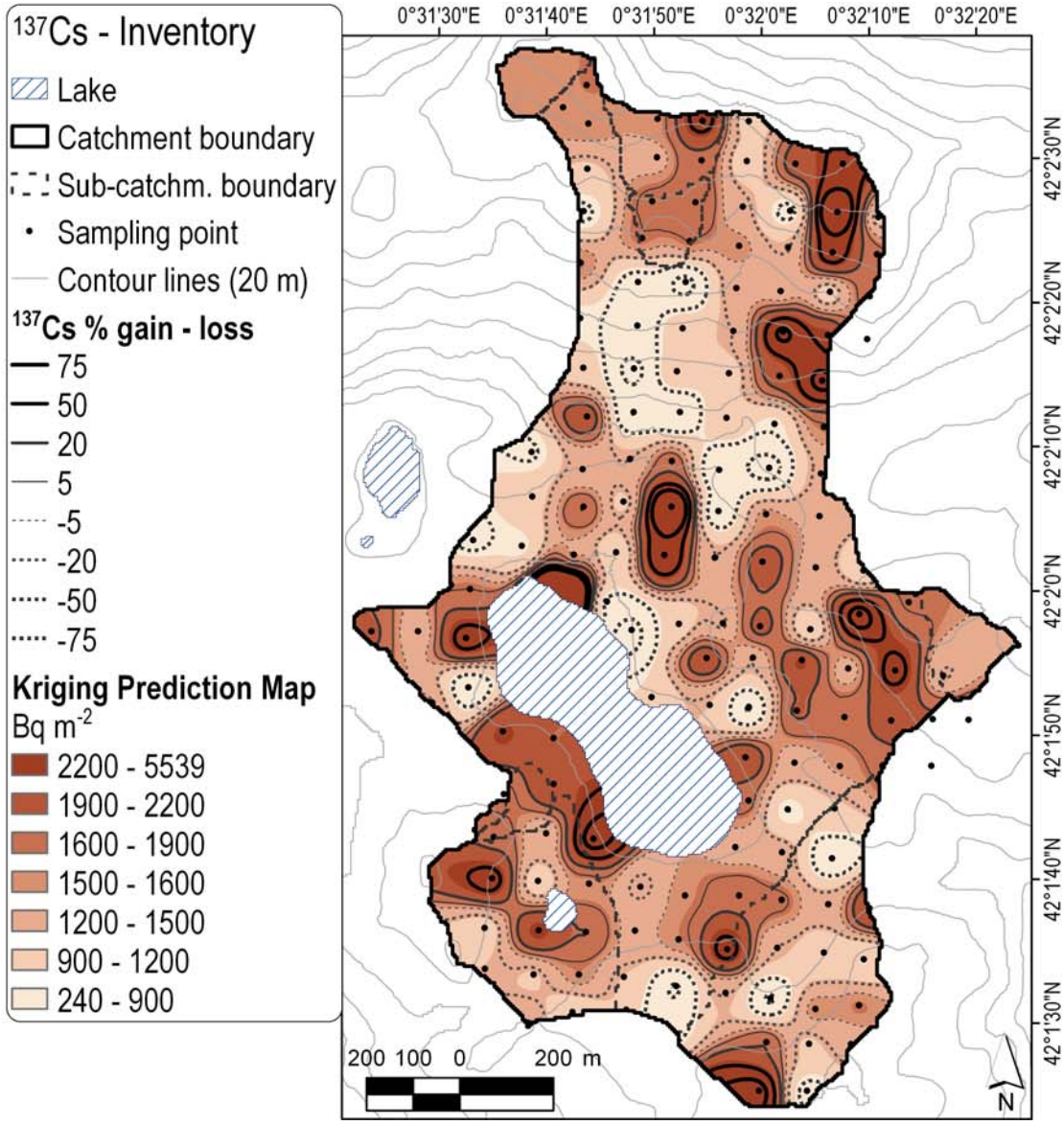
137Cs - Inventory
Lake
Catchment boundary
Sub-catchm. boundary
Sampling point
Contour lines (20 m)
137Cs % gain - loss
75
50
20
5
-5
-20
-50
-75
Kriging Prediction Map
Bq m-2
2200 - 5539
1900 - 2200
1600 - 1900
1500 - 1600
1200 - 1500
900 - 1200
240 - 900
0°31'30"E
0°31'40"E
0°31'50"E
0°32'0"E
0°32'10"E
0°32'20"E
42°2'30"N
42°2'20"N
42°2'10"N
42°2'0"N
42°1'50"N
42°1'40"N
42°1'30"N
200 100 0 200 m
N

Fig. 2

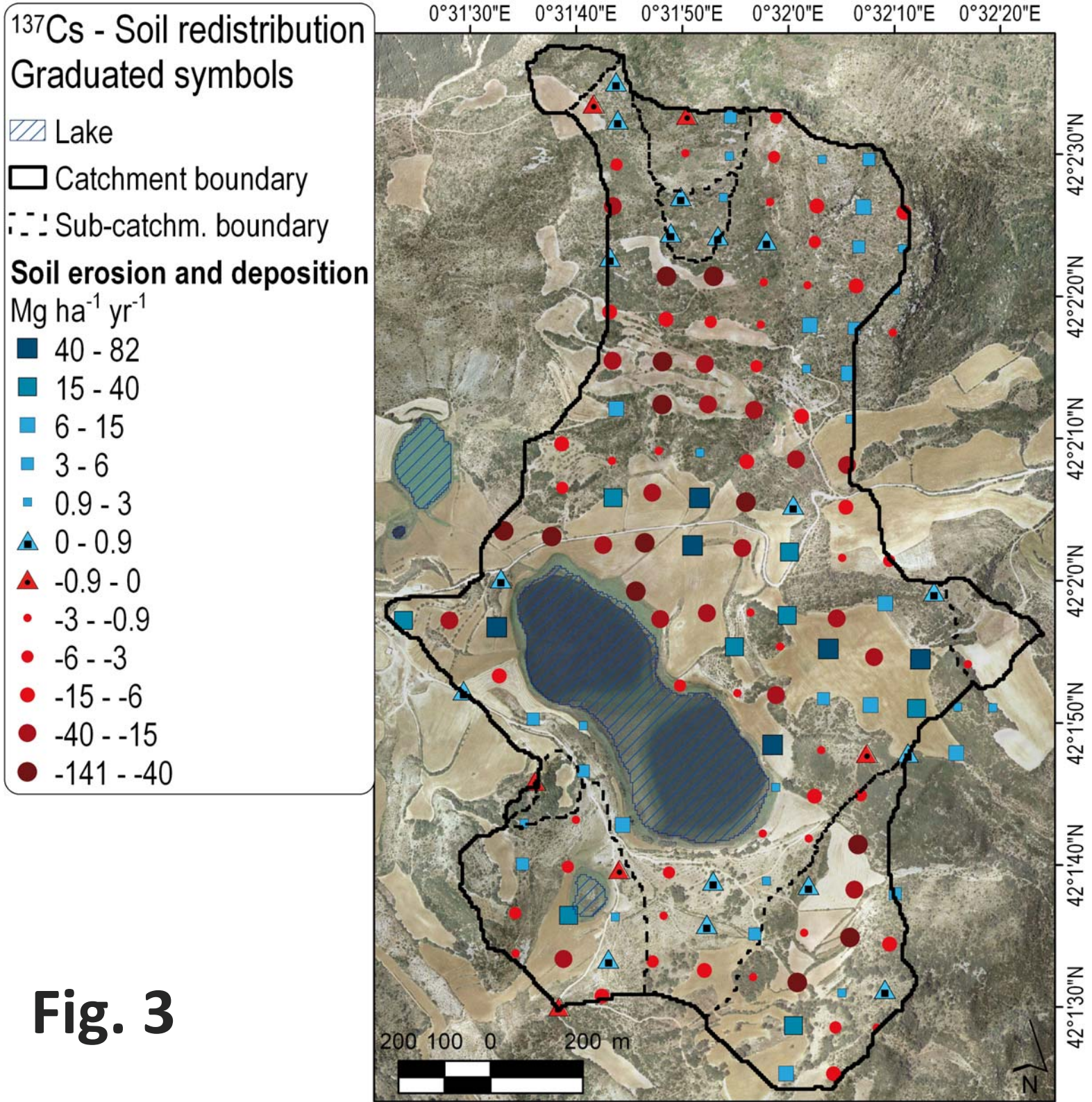
137Cs - Soil redistribution
Graduated symbols
Lake
Catchment boundary
Sub-catchm. boundary
Soil erosion and deposition
Mg ha-1 yr-1
40 - 82
15 - 40
6 - 15
3 - 6
0.9 - 3
0 - 0.9
-0.9 - 0
-3 - -0.9
-6 - -3
-15 - -6
-40 - -15
-141 - -40
0°31'30"E
0°31'40"E
0°31'50"E
0°32'0"E
0°32'10"E
0°32'20"E
42°2'30"N
42°2'20"N
42°2'10"N
42°2'0"N
42°1'50"N
42°1'40"N
42°1'30"N
200 100 0 200 m
N

Fig. 3

Fig. 4

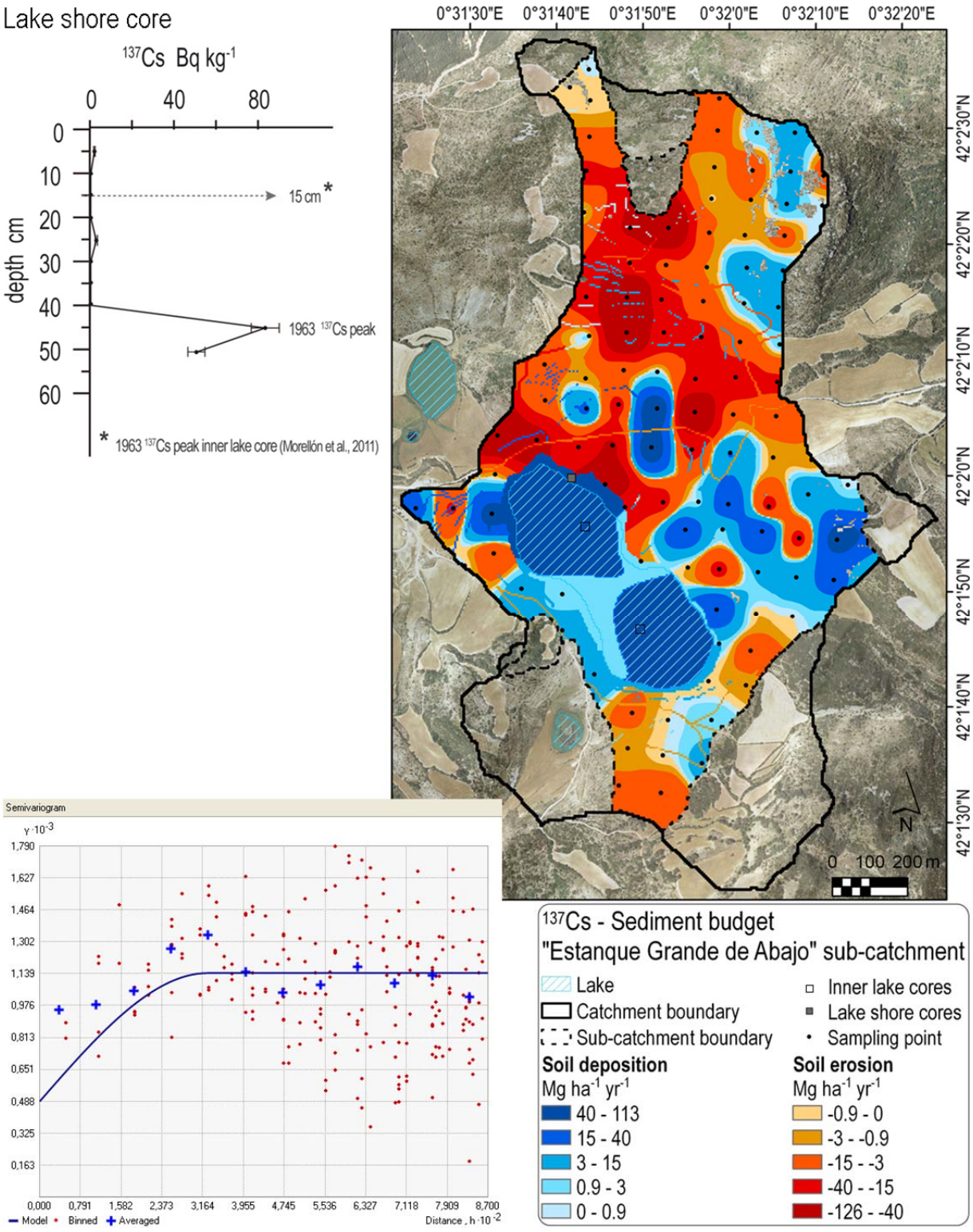
Lake shore core
137Cs Bq kg-1
0
40
80
depth cm
0
10
20
30
40
50
60
15 cm *
1963 137Cs peak
* 1963 137Cs peak inner lake core (Morellón et al., 2011)
0°31'30"E
0°31'40"E
0°31'50"E
0°32'0"E
0°32'10"E
0°32'20"E
42°2'30"N
42°2'20"N
42°2'10"N
42°2'0"N
42°1'50"N
42°1'40"N
42°1'30"N
N
0 100 200 m
Semivariogram
γ ·10-3
1,790
1,627
1,464
1,302
1,139
0,976
0,813
0,651
0,488
0,325
0,163
0,000
0,791
1,582
2,373
3,164
3,955
4,745
5,536
6,327
7,118
7,909
8,700
Model
Binned
Averaged
Distance , h ·10-2
137Cs - Sediment budget
"Estanque Grande de Abajo" sub-catchment
Lake
Catchment boundary
Sub-catchment boundary
Inner lake cores
Lake shore cores
Sampling point
Soil deposition
Mg ha-1 yr-1
40 - 113
15 - 40
3 - 15
0.9 - 3
0 - 0.9
Soil erosion
Mg ha-1 yr-1
-0.9 - 0
-3 - -0.9
-15 - -3
-40 - -15
-126 - -40

Fig. 5

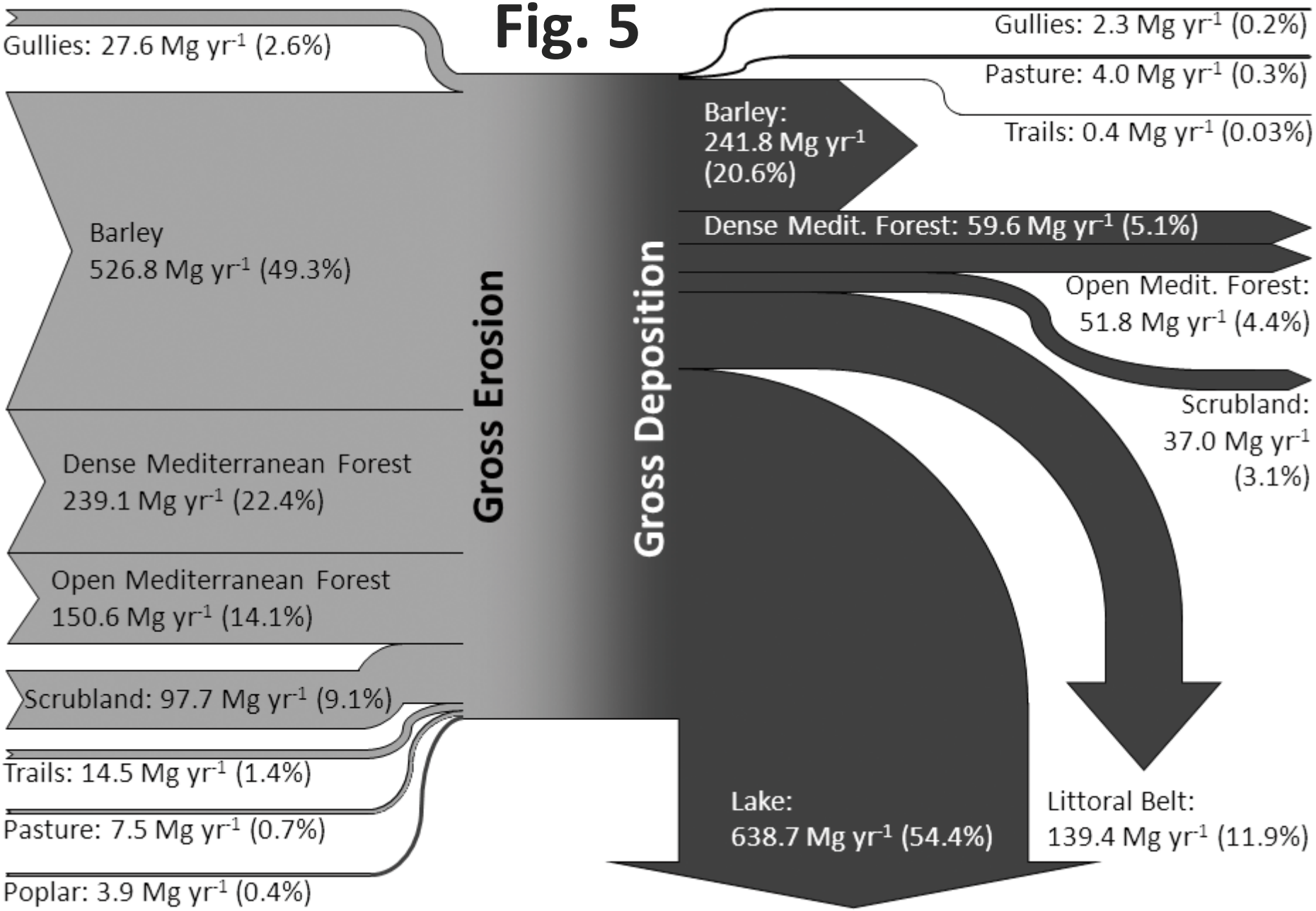
Gullies: 27.6 Mg yr-1 (2.6%)
Barley
526.8 Mg yr-1 (49.3%)
Dense Mediterranean Forest
239.1 Mg yr-1 (22.4%)
Open Mediterranean Forest
150.6 Mg yr-1 (14.1%)
Scrubland: 97.7 Mg yr-1 (9.1%)
Trails: 14.5 Mg yr-1 (1.4%)
Pasture: 7.5 Mg yr-1 (0.7%)
Poplar: 3.9 Mg yr-1 (0.4%)
Gross Erosion
Gross Deposition
Gullies: 2.3 Mg yr-1 (0.2%)
Pasture: 4.0 Mg yr-1 (0.3%)
Trails: 0.4 Mg yr-1 (0.03%)
Barley:
241.8 Mg yr-1
(20.6%)
Dense Medit. Forest: 59.6 Mg yr-1 (5.1%)
Open Medit. Forest:
51.8 Mg yr-1 (4.4%)
Scrubland:
37.0 Mg yr-1
(3.1%)
Lake:
638.7 Mg yr-1 (54.4%)
Littoral Belt:
139.4 Mg yr-1 (11.9%)